Nonlinear Crosstalk and Two Countermeasures in SCM–WDM Optical Communication Systems

Frank S. Yang, Michel E. Marhic, *Senior Member, IEEE, Member, OSA*, and Leonid G. Kazovsky, *Fellow, IEEE, Fellow, OSA*

***Abstract*—We investigate, theoretically and experimentally, crosstalk between wavelengths in subcarrier-multiplexed (SCM) wavelength-division multiplexed (WDM) optical communication systems. Crosstalk arises mainly from interactions between subcarriers on one wavelength and the optical carrier of another wavelength. In a dispersive fiber, crosstalk can be attributed to stimulated Raman scattering (SRS) and cross-phase modulation (XPM) combined with group velocity dispersion (GVD). We investigate the phase relationship between SRS-induced and XPM-induced crosstalks. Crosstalks induced by SRS and XPM add in the electrical domain and can interfere constructively or destructively. Experimental results show that the combined crosstalk level can be as high as 40 dBc after 25 km of SMF with two wavelengths and 18 dBm per wavelength of transmitted power. We propose two crosstalk countermeasures. The first countermeasure uses parallel fiber transmission. We show theoretically that both SRS-induced and XPM-induced crosstalks can be canceled to the first order. We present an experimental demonstration of concept which has achieved 15 dB of crosstalk cancellation over 200 MHz. The second countermeasure uses optical carrier suppression. We show, theoretically and experimentally, that by suppressing the optical carrier, we can significantly reduce crosstalk while maintaining the same link budget and carrier-to-noise ratio (CNR) at the receiver. 20 dB of crosstalk reduction over 2 GHz has been demonstrated experimentally.**

***Index Terms*—Cable television (CATV), cross-phase modulation (XPM), crosstalk, stimulated Brillouin scattering (SBS), subcarrier multiplexing (SCM), stimulated Raman scattering (SRS), wavelength-division multiplexing (WDM).**

I. Introduction

SUBCARRIER-MULTIPLEXED (SCM) optical systems have traditionally been used for cable television (CATV) distribution, backbones of wireless networks, and antenna remoting. With the explosion in the demand for access bandwidth, some of these systems are being upgraded to handle two-way communication of voice, video, and data through the addition of digitally modulated subcarriers and utilization of wavelength-division multiplexing (WDM). SCM–WDM is the predominant architecture for hybrid fiber-coax (HFC) system that is expected to compete with copper and fiber-to-the-home (FTTH) to provide services to the homes and businesses.

Manuscript received July 28, 1999. This work was supported by the National Science Foundation under Grant ECS-9417595

F. S. Yang was with 056 David Packard EE Building MC9515, Stanford University, Stanford, CA 94305 USA. He is now with the Core Switching Division, Ciena Corporation, Cupertino, CA 95014 USA.

M. E. Marhic and L. G. Kazovsky are with 056 David Packard EE Building MC9515, Stanford University, Stanford, CA 94305 USA.

Publisher Item Identifier S 0733-8724(00)03045-0.

When multiple wavelengths carrying SCM signals propagates in a single fiber, fiber nonlinearities can lead to crosstalk between subcarriers on different wavelengths. In a dispersive fiber, the dominant fiber nonlinearities that cause crosstalk are stimulated Raman scattering (SRS) and cross-phase modulation (XPM). SRS [1] and XPM [2] have previously been analyzed individually. Experimental results agree well with SRS for low modulation frequencies and large wavelengths separation [3], and XPM for high modulation frequencies and small wavelengths separation [4]. In this paper, we present and analyze a generalized expression for crosstalk, which includes the phase relationship between SRS-induced and XPM-induced crosstalks, that agrees well with experimental results for all ranges of modulation frequency and wavelength separation.

The crosstalk levels that have been predicted and measured to-date [1]–[4] indicate that crosstalk in SCM–WDM systems can easily reach intolerable levels, even with as few as two wavelengths. Theories on countermeasures using parallel and series techniques to cancel SRS-induced crosstalk have been presented in [5]. In this paper, we elaborate upon the parallel cancellation technique to show that it is effective against both SRS-induced and XPM-induced crosstalks. Experimental results are presented to support the claim. In addition, we present a more practical crosstalk reduction technique using optical carrier suppression.

The rest of this paper is organized as follows. Section II contains theoretical analysis and experimental investigation of nonlinear crosstalk caused by SRS and XPM, including their interaction. Section III describes and analyzes crosstalk cancellation using parallel fiber transmission and discusses the experimental results. Section IV describes and analyzes crosstalk reduction using optical carrier suppression and discusses the experimental results. Section V summarizes and concludes this paper.

II. Nonlinear Crosstalk in SCM–WDM Optical Communication Systems

When multiple wavelengths propagates in a single fiber, fiber nonlinearities can lead to interactions and crosstalk between wavelengths. These fiber nonlinearities are four-wave mixing (FWM), XPM, and SRS. Most hybrid fiber-coax (HFC) systems deployed today use standard single mode fiber (SMF) with zero-dispersion wavelength (λ_0) around 1310 nm. These HFC networks use SCM schemes with wavelengths near 1550 nm for low loss and IM–DD transmission/detection. As a result, typical dispersion in the fiber link is around 17 ps/km·nm. Because FWM efficiency degrades very quickly with increasing local dispersion, the FWM crosstalk in these SCM–WDM systems is

negligible. XPM affects only the phase of the signals and, in the absence of dispersion, does not affect IM–DD system. However, in the presence dispersion, the phase modulation is converted to intensity modulation leading to crosstalk. SRS contributes to crosstalk through Raman gain modulation and depletion.

This section first analyzes SRS-induced crosstalk and XPM-induced crosstalk separately. The interaction between them is then presented and verified against experimental work.

A. SRS-Induced Crosstalk

Consider two optical waves with the same polarization co-propagating in a single-mode fiber. The optical power at the input of the fiber can be expressed as

$$P_k = P_c(1 + m \cdot s(t)) \tag{1}$$

where

- k = 1 (λ_1) or 2 (λ_2) and
- $\lambda_1 > \lambda_2$;
- P_c is the average optical power;
- m is the modulation index;
- $s(t)$ is the modulating signal, which is assumed to be $\cos \Omega t$ where Ω is the subcarrier angular frequency.

We start with the coupled equations that describe SRS interaction in optical fiber [1], [6]

$$\frac{\partial P_1}{\partial z} + \frac{1}{V_{g1}} \frac{\partial P_1}{\partial t} = (gP_2 - \alpha) P_1 \tag{2}$$

$$\frac{\partial P_2}{\partial z} + \frac{1}{V_{g2}} \frac{\partial P_2}{\partial t} = (-gP_1 - \alpha) P_2 \tag{3}$$

where

- V_{gk} is the group velocity for the transmitted signal at λ_k;
- α is the fiber loss coefficient;
- g is the standard Raman gain coefficient divided by the fiber effective area ($g = g_R/A_{\text{eff}}$).

We first solve for P_1 in (2) by neglecting g. We then substitute P_1 into (3) to solve for P_2 to obtain [1]:

$$P_2(z, \tau_2) = P_2(0, \tau_2) e^{-\alpha z} \cdot \exp\left[-g \int_0^z P_1(0, \tau_2 + d_{21} z') e^{-\varepsilon z'} dz'\right] \tag{4}$$

where $d_{21} = (1/V_{g2} - 1/V_{g1})$ is the walkoff parameter, and $\tau_2 = t - z/V_{g2}$ (note that [1] is missing the $e^{-\alpha z'}$ term). For simplicity, we assume $P_1(0, \tau_1)$ to be of the form given by (1) and $P_2(0, \tau_2)$ to be unmodulated, $P_2(0, \tau_2) = P_c$. We expand the exponential in (4) to the first order in g and evaluate the integral to obtain:

$$P_2(z, \tau_2) = P_c e^{-\alpha z} \left(1 - gP_c \left(\frac{e^{-\alpha L} - 1}{\alpha}\right) - mgP_c \int_0^L \cdot e^{-\alpha z} \cos\left(\Omega \tau_2 + \Omega\, d_{21} z\right) dz\right). \tag{5}$$

The first term corresponds to the carrier power after fiber loss. The second term in the bracket corresponds to the interaction between the optical carriers, which falls at DC in the electrical domain. The third term is crosstalk. If $P_2(0, \tau_2)$ is also modulated, we would get interaction between the optical carrier of λ_1 and the subcarrier of λ_2. This corresponds to a power loss (or gain) due to SRS and does not contribute to crosstalk. We would also get an interaction between subcarriers of λ_1 and subcarriers of λ_2, generating second-order beat terms. These terms are proportional to m^2, and, because $m << 1$ in SCM systems, are typically negligible [1]. We keep only the crosstalk term in (5), evaluate the integral, normalize it by the magnitude of the modulation on $\lambda_1 \approx mP_c e^{-\alpha L}$, and express crosstalk in phasor notation:

$$xt_{\text{SRS2}} = \frac{gP_c}{\alpha - j\Omega\, d_{12}} \left[e^{-(\alpha - j\Omega\, d_{21})L} - 1\right] \tag{6}$$

where L is the length of the fiber. Expression (6) contains both magnitude and phase information. The phase refers to the electrical phase of the modulated signal relative to $\Omega\tau_2$. A similar expression can be obtained for crosstalk at λ_1:

$$xt_{\text{SRS1}} = \frac{-gP_c}{\alpha - j\Omega\, d_{12}} \left[e^{-(\alpha - j\Omega\, d_{12})L} - 1\right]. \tag{7}$$

The change in sign come from the fact that short wavelengths provide gain for long wavelengths through SRS; therefore λ_1 acquires crosstalk through gain, while λ_2 acquires crosstalk through depletion. The change in the walkoff parameter comes from the change in the reference wavelength ($d_{12} = -d_{21}$). The phase is now relative to $\Omega\tau_1$. Note that the magnitude of (7) remains the same as that of (6).

B. XPM-Induced Crosstalk

Consider two optical waves with the same polarization, co-propagating in a single-mode fiber as before. Let $A_k(z, t)$ denote the slowly varying complex field envelope of each wave, normalized so that $|A_k|^2 = P_k$. The coupled equations that describe XPM under the slowly varying-envelope approximation are [6]

$$\frac{\partial A_1}{\partial z} + \frac{1}{V_{g1}} \frac{\partial A_1}{\partial t} = \left(-i2\gamma P_2 - \frac{\alpha}{2}\right) A_1 \tag{8}$$

$$\frac{\partial A_2}{\partial z} + \frac{1}{V_{g^2}} \frac{\partial A_2}{\partial t} = \left(-i2\gamma P_1 - \frac{\alpha}{2}\right) A_2 \tag{9}$$

where γ is the nonlinearity coefficient. (Note the change in the sign of the complex term from [6] because we use the conventional $e^{j\omega t}$ notation, whereas [6] uses an $e^{-j\omega t}$ notation to represent time dependence). With the same initial condition as that of SRS at the fiber input, we obtain [7]

$$A_2(z, \tau_2) = A_2(0, \tau_2) e^{-\alpha z/2} \cdot \exp\left[-i2\gamma \int_0^z P_1(0, \tau_2 + d_{21} z') e^{-\varepsilon z'} dz'\right]. \tag{10}$$

At this point, crosstalk is entirely in the phase, $\varphi_2 = -2\gamma \int_0^z P_1(0, \tau_2 + d_{21} z') e^{-\varepsilon z'} dz'$. However, through group

velocity dispersion (GVD), the phase modulation is converted to intensity modulation via the relation [2], [8]

$$\frac{dP_2(z,\tau_2)}{dz} = -\ddot{\beta}_2 P_2(0,\tau_2)\, e^{-\alpha z}\frac{d^2\varphi_2(z,\tau_2)}{d\tau_2^2} \qquad (11)$$

where $\ddot{\beta}_2 = d^2\beta_2/d\omega^2$, and β_2 is the phase constant of λ_2. This is the incremental change in power over a small segment dz. Over the length L of the fiber, this incremental modulation will be attenuated by $e^{-\alpha(L-z)}$ due to fiber loss. We find the modulation at the end of the fiber by integrating $\int_0^L dP_2(z,\tau_2)\, e^{-\alpha(L-z)}$. To find crosstalk, we normalize by the magnitude of the modulation on $\lambda_1 \approx mP_c e^{-\alpha L}$, and express crosstalk in phasor notation

$$xt_{\mathrm{XPM2}} = \frac{-2\ddot{\beta}_2\Omega^2\gamma P_c}{(\alpha - j\Omega d_{21})^2}\left\{\left[e^{-\alpha L}\cos(\Omega d_{21}L) - 1 + \alpha L\right] + j\left[e^{-\alpha L}\sin(\Omega d_{21}L) - \Omega d_{21}L\right]\right\}. \qquad (12)$$

A similar expression can be obtained for crosstalk at λ_1

$$xt_{\mathrm{XPM1}} = \frac{-2\ddot{\beta}_1\Omega^2\gamma P_c}{(\alpha - j\Omega d_{12})^2}\left\{\left[e^{-\alpha L}\cos(\Omega d_{12}L) - 1 + \alpha L\right] + j\left[e^{-\alpha L}\sin(\Omega d_{12}L) - \Omega d_{12}L\right]\right\}. \qquad (13)$$

Unlike SRS-induced crosstalk, (12) and (13) have the same sign, and the only changes are: $d_{21} \to d_{12}$, $\ddot{\beta}_2 \to \ddot{\beta}_1$. The phases of (12) and (13) are relative to $\Omega\tau_2$ and $\Omega\tau_1$, respectively.

C. Total Crosstalk

Expressions (6), (7), (12), and (13) contain both phase and magnitude information. The total crosstalk power level in the electrical domain, normalized to the signal power level, can be expressed as

$$XT_k = |xt_{\mathrm{SRS}k} + xt_{\mathrm{XPM}k}|^2, \qquad k = 1, 2. \qquad (14)$$

For small Ω or large $\Delta\lambda = |\lambda_1 - \lambda_2|$, XT will be dominated by SRS. For large Ω or small $\Delta\lambda$, XT will be dominated by XPM. In between we must consider the phases of $xt_{\mathrm{SRS}k}$ and $xt_{\mathrm{XPM}k}$. It turns out that SRS-induced intensity modulation and the XPM-induced optical phase modulation are exactly in-phase or exactly 180° out-of-phase, depending on k and the sign of $\ddot{\beta}_k$. When the optical phase modulation is converted to intensity modulation via GVD, its phase will change somewhat but remain relatively close. As a result, assuming $\lambda_1 > \lambda_2$, $xt_{\mathrm{SRS}k}$ and $xt_{\mathrm{XPM}k}$ will add in-phase when $k = 1$ and out-of-phase when $k = 2$ [9], because $xt_{\mathrm{SRS}k}$ changes sign with k, while $xt_{\mathrm{XPM}k}$ does not.

To illustrate the point, Fig. 1(a) shows a plot of the theoretical crosstalk level at λ_1 versus modulation frequency, $f = \Omega/2\pi$, for $\Delta\lambda = 4$ nm, $P_c = 17$ dBm, and $L = 25$ km. The solid line denotes the total crosstalk, and the dashed lines denote the magnitudes of the individual contributions from SRS and XPM, respectively. We clearly see the dominance of SRS at the low frequency, and of XPM at the high frequency. Where the dashed curves cross, we see that the total crosstalk is 6 dB higher than the individual contributions, indicating that $xt_{\mathrm{SRS}k}$ and $xt_{\mathrm{XPM}k}$ add nearly in phase.

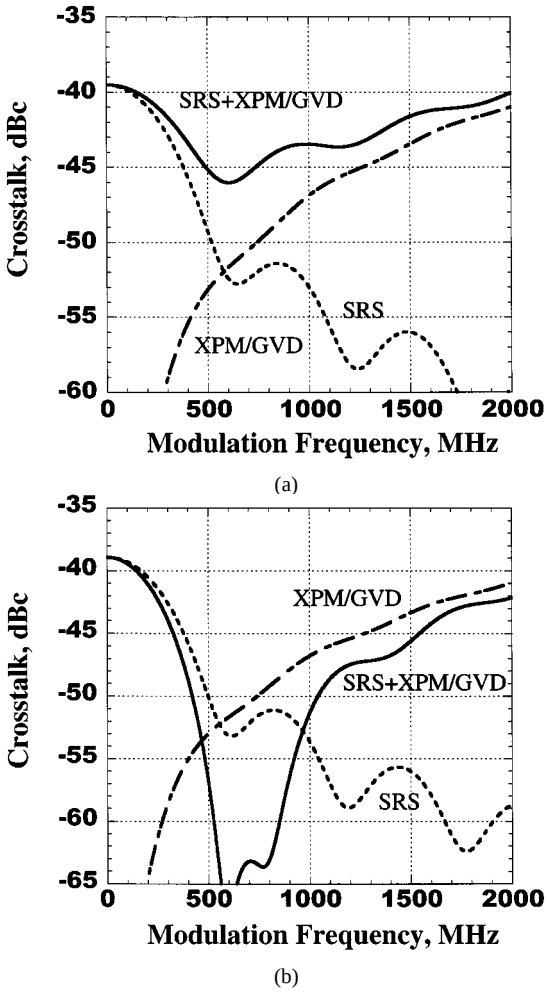

Fig. 1. Theoretical crosstalk level versus modulation frequency at (a) λ_1 and (b) λ_2 for $\Delta\lambda = 4$nm, $P_c = 17$ dBm, and $L = 25$ km. The solid line denotes the total crosstalk and the dashed lines denote the individual contribution from SRS and XPM.

Fig. 1(b) shows a plot of the theoretical crosstalk level at λ_2 for the same $\Delta\lambda$. The magnitude of the individual contributions from SRS and XPM remain the same. However, because the SRS crosstalk is now through depletion rather than gain, its phase changes by π, and thus we have a cancellation between SRS-induced and XPM-induced crosstalks.

D. Experiment

We measure experimentally the dependence of crosstalk on modulation frequency, wavelength separation, and transmit power level. The setup is shown in Fig. 2. A DFB laser, henceforth called the pump, is externally modulated with a tunable single tone by an external Mach–Zehnder (MZ) modulator. The output of the pump is combined with the output of an unmodulated tunable external cavity laser, henceforth called the probe, via a 3-dB coupler. A phase modulator dithers the optical phase with a 1-GHz pseudorandom bit stream (PRBS) to suppress stimulated Brillouin scattering (SBS). The two wavelengths are amplified by an erbium-doped fiber amplifier (EDFA) and passed through 25 km of standard SMF with $\alpha = 0.22$, $D = 17$ ps/nm/km (at 1550 nm), and $\gamma = 0.95 \times 10^{-3}$/(m·W). A tunable Fabry–Perot filter selects which wavelength will

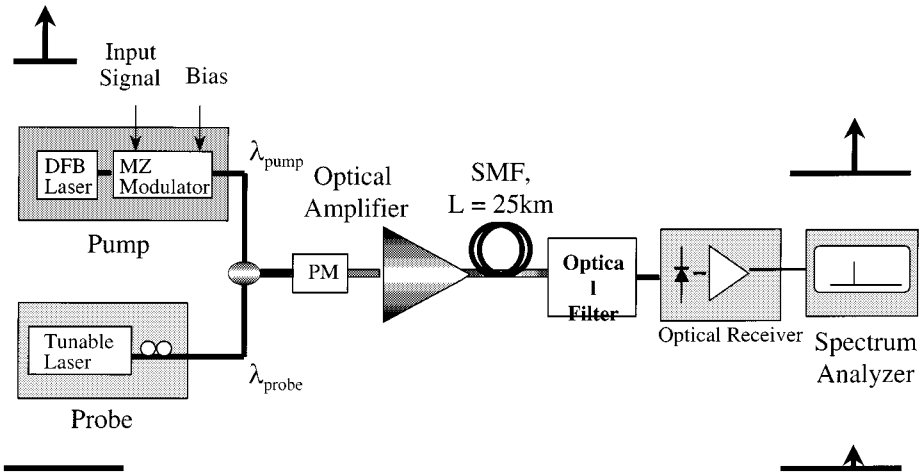

Fig. 2. Experimental setup for crosstalk measurement.

be received by the optical receiver. An electrical spectrum analyzer measures the power level at f. Crosstalk is measured by comparing the received electrical power of the pump and that of the probe at f (the optical receiver receives the same optical power at either wavelength). Since the theory assumes same polarization for the two wavelength, we use a polarization controller at the probe to align its polarization to the pump.

Fig. 3(a) shows the measured crosstalk level versus modulation frequency for $\lambda_{\rm pump} = 1542$ nm, $\lambda_{\rm probe} = 1546$ nm, and $P_c = 16.8$ dBm. The solid line corresponds to theory, and the dots are experimental data points. As predicted in theory, SRS and XPM add in phase. Fig. 3(b) shows the measured crosstalk level versus modulation frequency for $\lambda_{\rm pump} = 1542$ nm, $\lambda_{\rm probe} = 1552$ nm, and $P_c = 18.2$ dBm. Because of the larger $\Delta\lambda$, SRS is enhanced while XPM is mitigated. Fig. 3(c) shows the measured crosstalk level versus f for $\lambda_{\rm pump} = 1554$ nm, $\lambda_{\rm probe} = 1541$ nm, and $P_c = 16.5$ dBm. In this case, because $\lambda_{\rm probe} < \lambda_{\rm pump}$, $xt_{{\rm SRS}k}$ and $xt_{{\rm XPM}k}$ add out of phase, and they cancel almost exactly at about 1540 MHz. The match between experiments and theory is good. The variations can be attributed to polarization drift and drift in the bias of the MZ modulator.

Fig. 4(a) shows the crosstalk level versus P_c, at a fixed $f = 55.5$ MHz for three $\Delta\lambda$'s. Because SRS dominates at this frequency, crosstalk increases with increasing $\Delta\lambda$, as we expect. It will continue to increase with increasing $\Delta\lambda$ up to 100 nm (SRS gain peak) before falling. Versus the horizontal axis, the crosstalk level varies as P_c^2 (slope $= 2$ in dB–dB scale), regardless of $\Delta\lambda$. Fig. 4(b) shows the result of the same experiment, but with a fixed $f = 1.9$ GHz, where XPM dominates. The power dependence remains the same. However, the crosstalk level now decreases with increasing $\Delta\lambda$ because increased group velocity walkoff reduces XPM.

III. Countermeasure 1: Crosstalk Cancellation Using Parallel Fiber Transmission

Now that we have thoroughly investigated the crosstalk mechanisms in SCM–WDM systems, we propose countermeasures to combat crosstalk. This section discusses a countermeasure using parallel fiber transmission. This technique is theoretically elegant, but experimentally difficult to attain. We will first describe the technique and its theoretical limitations. We will then present an experimental demonstration and discuss practical limitations.

A. Theory

The idea of crosstalk cancellation is straightforward. If we could transmit the same set of signals on two fibers and then combine them at the receiver, we could arrange the parameters in such a way that crosstalks from the two fibers will cancel, while signals will add [5]. The detailed arrangement of the system is as follows.

Let s_1 and s_2 denote signals transmitted on λ_1 and λ_2, respectively, through fiber F. Let s_1' and s_2' denote signals transmitted on λ_1' and λ_2', respectively, through fiber F'. We let $s_1' = s_2$, $s_2' = s_1$, and $\lambda_1 - \lambda_2 = \lambda_1' - \lambda_2'$. We further assume, for the wavelengths of interest, that $L = L'$, $g = g'$, $\gamma = \gamma'$, $\alpha = \alpha'$, and $D = -D'$ where $'$ denotes variables in F'. The condition on fiber dispersion can be met by using fibers with reverse dispersion characteristics [10] or operating λ_k and λ_k' on opposite sides of the zero-dispersion wavelength of the same type of fiber. After L km of transmission, crosstalks on λ_1 in F and λ_2' in F' are given by

$$xt_1 = xt_{\rm SRS1} + xt_{\rm XPM1} xt_2' = xt_{\rm SRS2}' + xt_{\rm XPM2}' \qquad (15)$$

where $xt_{\rm SRS1}$ and $xt_{\rm XPM1}$ are given by (7) and (13), and $xt_{\rm SRS2}'$ and $xt_{\rm XPM2}'$ are given by (6) and (12), respectively. Because $\lambda_1 - \lambda_2 = \lambda_2' - \lambda_1'$, $d_{12} = d_{21}'$; and because $D = -D'$, $\dot\beta_1 = -\dot\beta_2$'. As a result, we have $xt_{\rm SRS1} = -xt_{\rm SRS2}'$, $xt_{\rm XPM1} = -xt_{\rm XPM2}'$, and $xt_1 = -xt_2'$. Since the phases of xt_1 and xt_2' are measured relative to s_1 and s_2', respectively, xt_1 and xt_2' will necessarily have equal magnitudes and be 180° out-of-phase if we ensure that s_1 and s_2' have the same phases. The phases of s_1 and s_2' can be adjusted by inserting fiber lengths after wavelength demultiplexing, or more easily by delaying the phases in the electrical domain after detection to compensate for GVD. Finally, by combining the received signals from the two paths, we achieve exactly what we set out to do: add the signals and cancel crosstalks. The same argument applies to s_2, s_1', xt_2, and xt_1' as well.

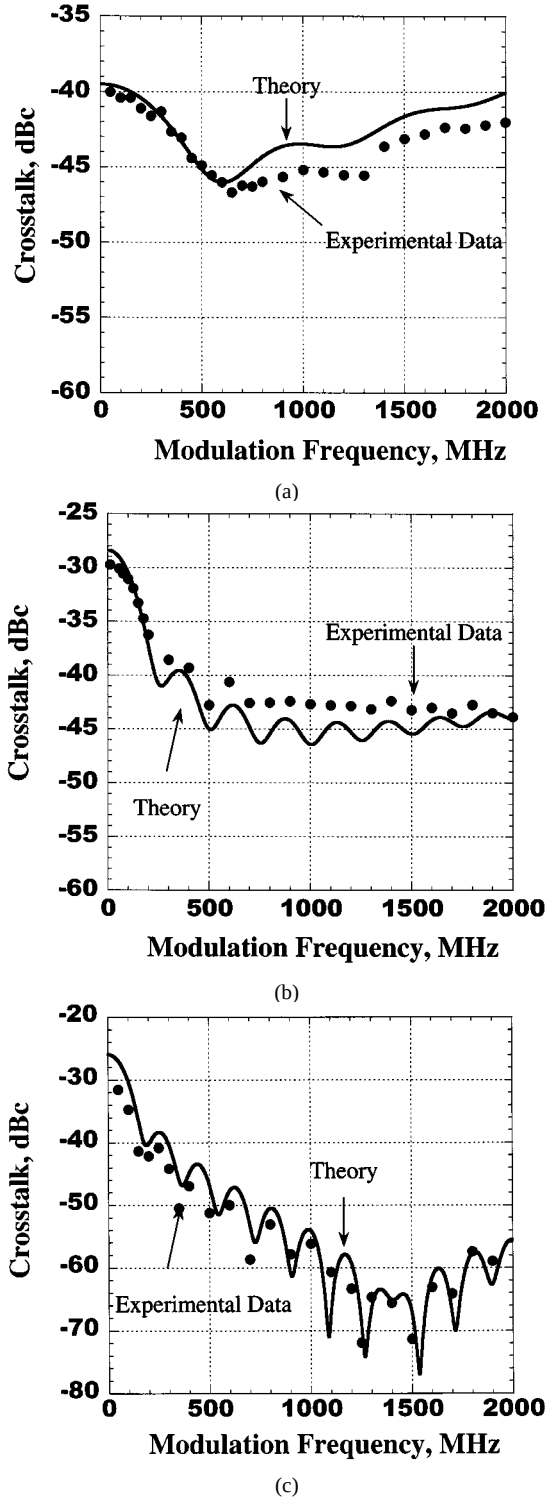

Fig. 3. Measured crosstalk level versus modulation frequency for (a) $\lambda_{\rm pump} =$ 1542 nm, $\lambda_{\rm probe} =$ 1546 nm, and $P_c =$ 16.8 dBm; (b) $\lambda_{\rm pump} =$ 1542 nm, $\lambda_{\rm probe} =$ 1552 nm, and $P_c =$ 18.2 dBm; and (c) $\lambda_{\rm pump} =$ 1554 nm, $\lambda_{\rm probe} =$ 1541 nm, and $P_c =$ 16.5 dBm. The solid line corresponds to theory, and the dots are experimental data points.

Note that we derived the expression for crosstalk only to the first order in g and $\ddot{\beta}$. The crosstalk cancellation, therefore, is exact only to the first order as well [5]. However, since g and $\ddot{\beta}$ are typically very small numbers, residual crosstalk from higher order contributions are typically negligible.

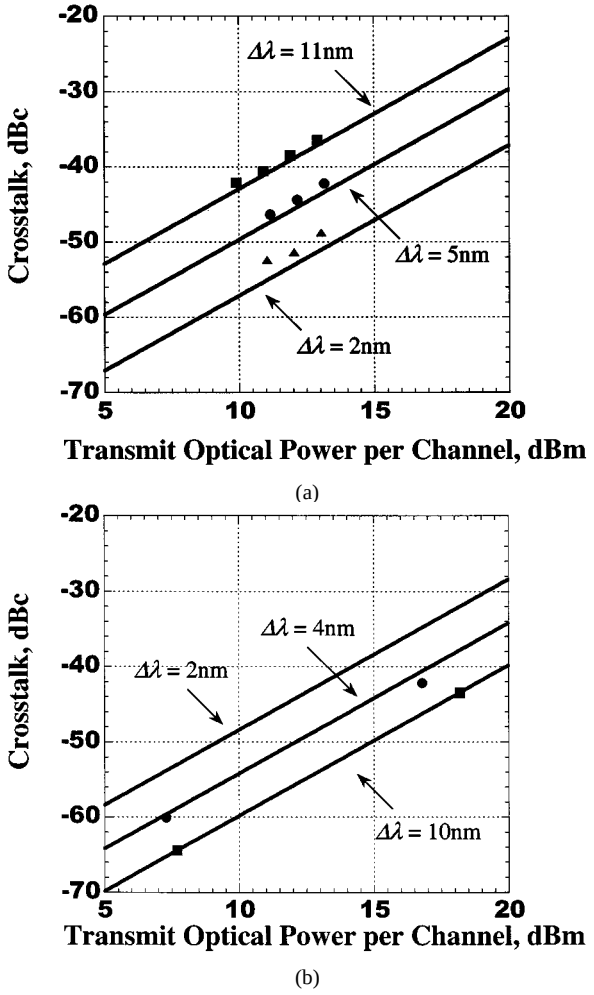

Fig. 4. Measured crosstalk level versus transmitted optical power per channel (P_c), at a fixed modulation frequency of (a) 55.5 MHz and (b) 1.9 GHz. The solid lines correspond to theory and the dots are experimental data points.

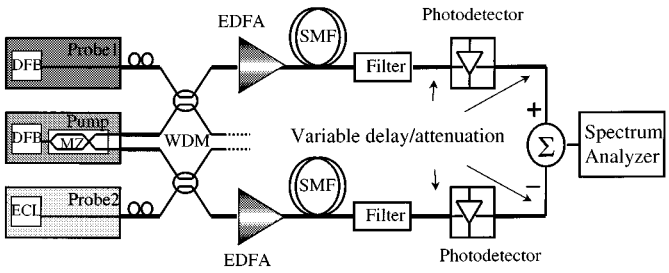

Fig. 5. Experimental setup for crosstalk cancellation using parallel transmission.

B. Experiment

The experimental setup for crosstalk cancellation is shown in Fig. 5. A pump laser (DFB) is modulated by an external MZ modulator with dual outputs. Each output is coupled to an unmodulated probe laser (DFB or ECL), amplified by an EDFA, and transmitted over 25 km of SMF with $\alpha = 0.22$, $D =$ 17 ps/nm/km, and $\gamma = 0.95 \times 10^{-3}$/(m·W). The transmitted power into each fiber is 14 dBm/wavelength. The wavelengths of the probes are 8 nm above and below the pump wavelength, respectively. Fabry–Perot filters select the probe wavelengths at

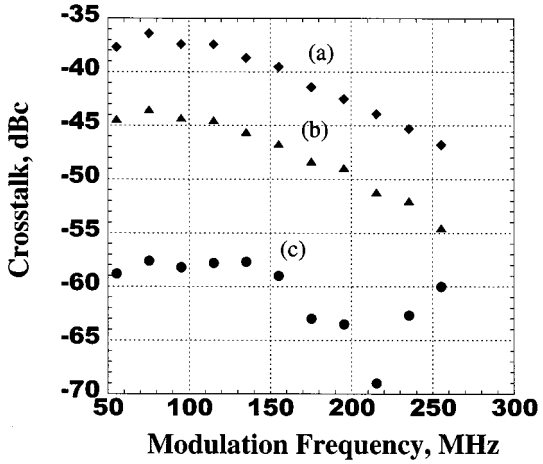

Fig. 6. Measured crosstalk level versus modulation frequency for (a) crosstalk at F; (b) crosstalk at F'; and (c) crosstalk after cancellation.

each fiber. The probes are then converted to the electrical domain and combined using Harmonic Lightwaves' lightwave extender [11]. Fiber segments and coaxial segments are used to fine-adjust the total path lengths for optimal cancellation. The polarization of the probes are manually adjusted to align with the pump polarization.

There are two major discrepancies between the experimental setup and the theoretical system described earlier. First, the outputs of the MZ modulator have 180° phase difference, thus violating our assumption that $s_1 = s_2'$. We compensate for this by performing a subtraction of the received signals instead of an addition. Second, and perhaps the most serious experimental limitation, is the absence of reverse-dispersion fiber in our system. D in both of our fibers have positive signs, and we are not able to operate at two sides of the zero-dispersion wavelength. This is a major violation of the our theoretical assumption. The consequences are twofold. First, the cancellation of $xt_{\rm SRS}$ will be imperfect because $d_{12} \neq d_{21}'$. However, since the transmission length is relatively short, we may still achieve good cancellation especially at small Ω. Second, because $\ddot{\beta}_1 \neq -\ddot{\beta}_2$', $xt_{\rm XPM}$ will not cancel, and in fact will add, though not exactly in phase because $d_{12} \neq d_{21}'$.

Fig. 6 shows the measured crosstalk level versus modulation frequency for (a) crosstalk at F; (b) crosstalk at F'; and (c) crosstalk after cancellation. Although crosstalks at F and F' have different relative magnitude in dBc, the absolute magnitudes in dBm are adjusted to be equal at the combiner. In Fig. 6(a) and (b), crosstalks are dominated by SRS in the frequency range shown. In Fig. 6(c), we clearly see the cancellation of these SRS-induced crosstalks, reducing the total crosstalk level by about 20 dB for frequencies below 210 MHz. At the same time, however, the XPM-induced crosstalks are adding instead of canceling. Beyond 210 MHz, $|xt_{\rm XPM}|$ surpasses the residual $|xt_{\rm SRS}|$ to dominate the total crosstalk. Subsequent rise in the crosstalk level beyond 210 MHz matches very well with the theoretical prediction of $|xt_{\rm XPM}|$ alone.

Although the experiment lacked a key component, namely reverse-dispersion fiber, to achieve broadband cancellation, the outcome still validates our theory and demonstrates the feasibility of such cancellation method. It also provides another verification of the crosstalk phases. Reverse-dispersion fibers are available today in several research institutes [10] and are becoming more readily available commercially. By using such fibers, one should be able to obtain a much better verification of the proposed cancellation technique.

IV. Countermeasure 2: Crosstalk Reduction Using Optical Carrier Suppression

The parallel technique takes advantage of the phase relationship between crosstalks and signals to achieve cancellation. This next countermeasure works directly on the magnitude of crosstalk to achieve crosstalk reduction. It utilizes optical carrier suppression, which has previously been used in millimeter-wave (mm-wave) systems to increase dynamic range. We will first show theoretically how optical carrier suppression can reduce crosstalk. We will then present experimental results and discuss limitations.

A. Theory

The theory for crosstalk reduction using optical carrier suppression is quite straightforward. From (14), we know that XT varies in a complex way with $\Delta\lambda$, D, and Ω. However the variation of XT with P_c is simple: $XT \propto P_c^2$.

Most SCM optical communication links operate with high transmitted power, P_c, in order to maintain good CNR on all subcarriers. However m is kept at a few percent in order to maintain high linearity. As a result, most of the transmitted optical power resides in the optical carrier power, which contains no useful information. Suppressing this optical carrier has been shown to effectively increase the modulation depth without sacrificing linearity [12], and [13]. It also allows us to maintain the same CNR while reducing P_c.

To quantify this analytically, we assume the transmitted optical signal to be of the form given in (1) in the tradition system. Suppose, in the suppressed-carrier system, we reduce the transmitted power by a factor a so that the transmitted optical signal is given by

$$P_k = aP_c(1 + m' \cdot s(t)),\ k = 1, 2 \tag{17}$$

where m' is the new modulation index after carrier suppression. In a real system, a and m' can be adjust independently of one another: m' through optical carrier suppression, and a through EDFA gain or external attenuator. At the receiver, after conversion to the electrical domain, the signal power level is proportional to $(mP_c)^2$ for the tradition system, and proportional to $(am'P_c)^2$ for the suppressed-carrier system. If we let $m' = m/a$, then the signal power level is the same for both system. If the substitute (17) into the derivation for XT, basically replacing all $P_c's$ by (aP_c)'s, we find from (14) that

$$XT_{\text{suppressed-carrier}} = a^2 XT_{\text{traditional}}. \tag{18}$$

This point is illustrated in Fig. 7.

B. Experiment

There are several ways to achieve optical carrier suppression. The most straightforward method is to use a narrow-band optical

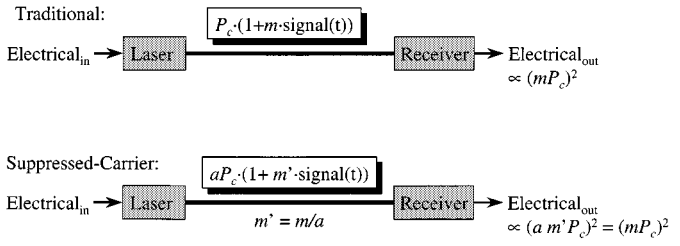

Fig. 7. Illustration of how carrier suppression can reduce transmitted optical power while maintaining the same received electrical signal level.

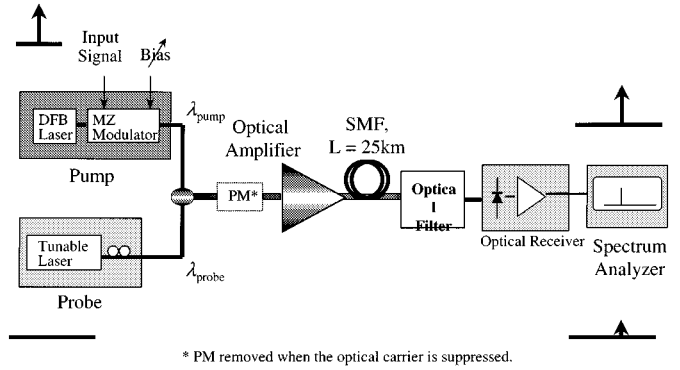

Fig. 8. Experimental setup for crosstalk reduction using optical carrier suppression.

notch filter to filter away the optical carrier. However when the subcarriers are within tens of megahertz from the optical carrier, such filters are practically nonexistent. The best-performance, but probably the most complicated, method is to use optical carrier cancellation, usually in a loop mirror, where an unmodulated carrier cancels a modulated carrier [14]. The suppression can be very efficient. However, for our application, we want to have enough optical carrier left at the receiver to perform direct detection. We've chosen a third method of optical carrier suppression: using low-biasing of an MZ modulator [13]. This is very simple to implement experimentally, and the level of suppression can be easily controlled. While low-biasing a MZ modulator does not add to the third-order nonlinearity of the modulator, it does increase the second-order nonlinearity significantly. In a real system, this would require operation of the subcarriers to within an octave so that all second-order harmonics and beat terms fall out-of-band.

The experimental setup is shown in Fig. 8. It is essentially the same setup as that of Fig. 2, with two differences. First, the bias voltage to the MZ modulator is now variable so that we can adjust the level of optical carrier suppression. Second, the phase modulator, used for SBS suppression, can be removed when the transmitted optical power level is suppressed below the SBS threshold. We adjust the bias of the MZ modulator and the gain of the EDFA to reduce P_c by 10 dB. The residual optical carrier is strong enough that direct detection can still be employed. Because of the increase in modulation depth by a factor of 10 arising from the suppressed carrier, the received electrical power remains the same. We maintain equal optical power for both wavelengths at the output of the EDFA.

Fig. 9(a) and (b) shows the measured crosstalk levels after optical carrier suppression with $\Delta\lambda = 4$ nm and $\Delta\lambda = 10$ nm,

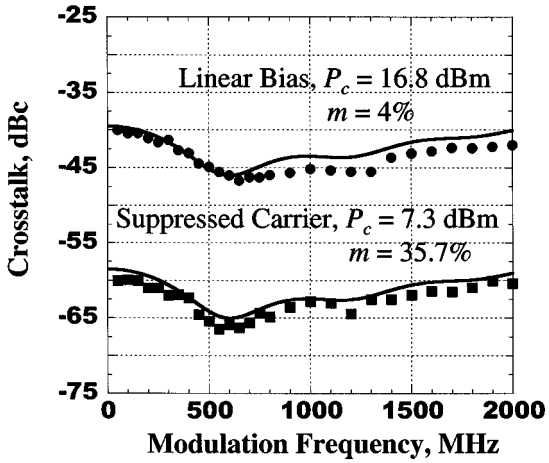

(a)

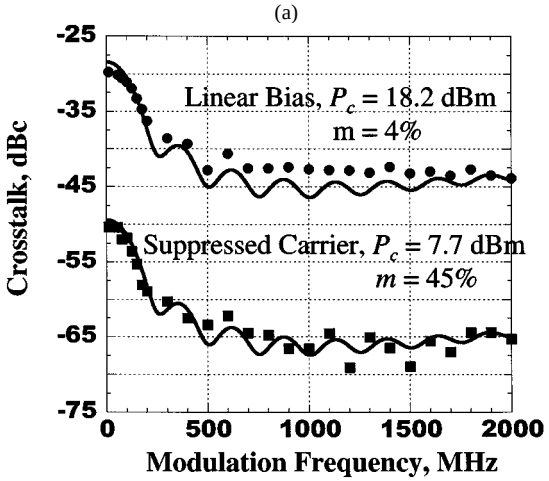

(b)

Fig. 9. Measured crosstalk before and after optical carrier suppression for (a) $\Delta\lambda = 4$ nm and (b) $\Delta\lambda = 10$ nm.

respectively. For comparison, we repeat Fig. 3(a) and (b) (crosstalk under normal bias for the same parameters) on the same plots. We see that a decrease of 10 dB in P_c results in a decrease in crosstalk of 20 dB as predicted by theory. This is true in the SRS-dominated regime as well as the XPM-dominated regime. Fig. 10(a) shows the electrical spectrum of the received signal under normal bias. Because of the 1-GHz PRBS necessary to suppress SBS, we see a very high noise floor from the residual amplitude modulation of the phase modulator, and from phase-to-intensity conversion through fiber GVD. Fig. 10(b) shows the electrical spectrum of the received signal when the optical carrier is suppressed. The transmitted optical power is now below the SBS threshold so that the phase dithering can be removed from the system. We see that the received signal level is the same as that of Fig. 10(a), indicating that we have not lost any link budget due to carrier suppression or SBS. Furthermore, the noise floor is dramatically lowered in the absence of the 1-GHz PRBS phase dithering, leading to increased CNR.

This experiment demonstrates the applicability of optical carrier suppression in reducing crosstalk. Several practical issues need to be addressed before this technique can be applied to a real system. The first is the problem of single-octave operation. This is actually not a new limitation to SCM optical system, and

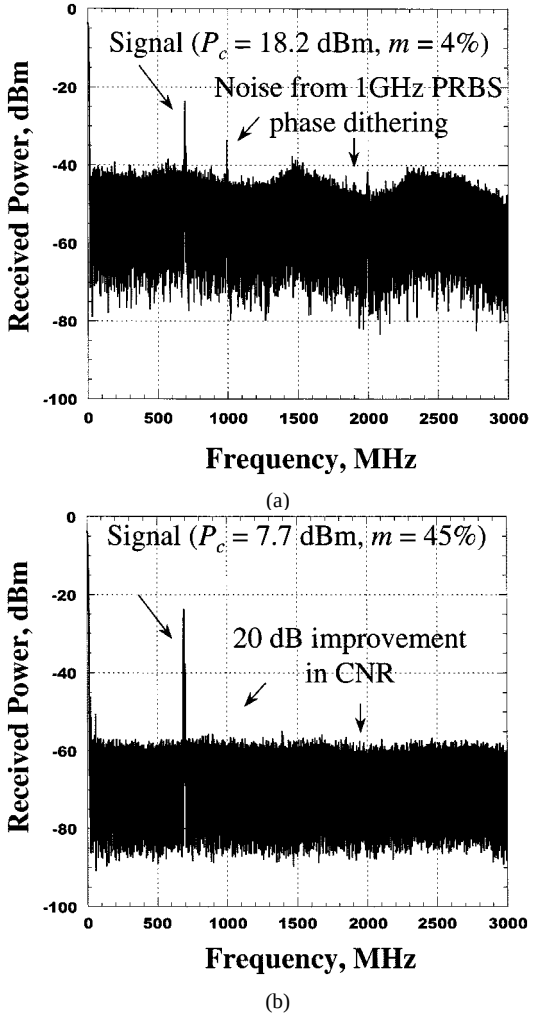

Fig. 10. Electrical spectrum of received signal under (a) normal bias with phase dithering for SBS suppression and (b) low bias output phase modulation.

even some of the deployed systems today operate within one octave [15]. Note, however, that this limitation comes from low-biasing of the MZ modulator, and not from optical carrier suppression in general. Other optical carrier suppression methods, such as the ones described earlier in this section, will not induce second-order distortion. The price to pay is usually added system complexity. The second problem, more specific to optical carrier suppression, is the limitation on the number of subcarriers due to clipping [16] because of the increased modulation index per channel. Several clipping reduction techniques have been proposed [17], and [18] and can be used. Alternatively, we can add the optical carrier back at the receiver, or increase the bitrate per subcarrier to compensate for decreased number of carriers.

V. Summary and Conclusion

We have investigated, theoretically and experimentally, optical crosstalk arising from SRS and XPM in SCM–WDM optical systems. We have analyzed the phase as well as the magnitude of crosstalk. In general, SRS-induced crosstalk dominates at low modulation frequency and large wavelength separations, and XPM-induced crosstalk dominates at high modulation frequency and short wavelength separation. If the pump wavelength is shorter than the probe wavelength, SRS-induced and XPM-induced crosstalks will add in electrical amplitude. If the pump wavelength is longer than the probe wavelength, then they will cancel.

We use the phase and magnitude relations of crosstalk to design two countermeasures. In the parallel transmission technique, we take advantage of the phase dependence on dispersion and pump/probe relationship to achieve cancellation. By transmitting the same set of signals over two equal-length fibers, we have shown, theoretically and experimentally, that we can add the signals and cancel crosstalks simultaneously at the receiver. 20 dB of carrier suppression has been demonstrated over 200-MHz bandwidth.

In the optical carrier suppression technique, we take advantage of the magnitude dependence of crosstalk on the transmitted carrier power, P_c. By reducing P_c through carrier suppression, we have shown theoretically and experimentally that crosstalk can be reduced while received signal level remains the same. Furthermore, we have shown that phase dithering for SBS suppression can be removed when the optical carrier is suppressed to increase the received CNR. 20 dB of carrier suppression has been demonstrated over 2 GHz bandwidth.

Both countermeasures can achieve wide-band crosstalk cancellation or reduction. The advantage of countermeasure 1 is that crosstalk can, in theory, be canceled exactly to the first order, regardless of the magnitude of crosstalk. Furthermore receiver sensitive increases by 3 dB from the addition of signals from two path. The drawbacks are in system complexity, equal fiber length requirement, and the need for reverse-dispersion fiber. The advantages of countermeasure 2 are in simplicity and the removal of SBS suppression phase/frequency dithering. The level of crosstalk can be reduced significantly over all frequencies, but the shape of the crosstalk spectrum will remain the same. The drawbacks are in single-octave operation (if using low-biasing of MZ modulator) and increased clipping effect. Both drawbacks have remedies at the cost of system complexity.

Acknowledgment

The authors would like to acknowledge the generous loan of equipment and space by Harmonic Lightwaves for portions of these experiments.

References

[1] Z. Wang, A. Li, C. J. Mahon, G. Jacobsen, and E. Bodtker, "Performance limitations imposed by stimulated Raman scattering in optical WDM SCM video distribution systems," *IEEE Photon. Technol. Lett.*, vol. 7, pp. 1492–1494, Dec. 1995.

[2] Z. Wang, E. Bodtker, and G. Jacobsen, "Effects of cross-phase modulation in wavelength-multiplexed SCM video transmission systems," *Electron. Lett.*, vol. 31, no. 18, pp. 1591–1592, Aug. 1995.

[3] A. Li, C. J. Mahon, Z. Wang, G. Jacobsen, and E. Bodtker, "Experimental confirmation of crosstalk due to stimulated Raman scattering in WDM AM-VSB CATV transmission systems," *Electron. Lett.*, vol. 31, no. 18, pp. 1538–1539, Aug. 1995.

[4] R. Hui, Y. Wang, K. Demarest, and C. Allen, "Frequency response of cross-phase modulation in multispan WDM optical fiber systems," *IEEE Photon. Technol. Lett.*, vol. 10, pp. 1271–1273, Sept. 1998.

[5] M. E. Marhic, F. S. Yang, and L. G. Kazovsky, "Cancellation of stimulated-Raman-scattering crosstalk in wavelength-division-multiplexed optical communication systems by series or parallel techniques," *J. Opt. Soc. Amer. B*, vol. 15, no. 3, pp. 957–963, Mar. 1998.
[6] G. P. Agrawal, *Nonlinear Fiber Optics*, 2nd ed. New York: Academic., 1995.
[7] T. K. Chiang, N. Kagi, M. E. Marhic, and L. G. Kazovsky, "Cross-phase modulation in fiber links with multiple optical amplifiers and dispersion compensators," *J. Lightwave Technol.*, vol. 14, pp. 249–260, Mar. 1996.
[8] K. Peterman, "FM–AM noise conversion in dispersive single-mode fibre transmission lines," *Electron. Lett.*, vol. 26, no. 25, pp. 2097–2098, Dec. 1990.
[9] M. R. Phillips and D. M. Ott, "Crosstalk due to optical fiber nonlinearity in WDM CATV lightwave systems," in *Proc. OFC '99*, San Diego, CA, Feb. 1999, pp. 227–229.
[10] K. Mukasa, Y. Akasaka, Y. Suzuki, and T. Kamiya, "Novel network fiber to manage dispersion at 1.55 μm with combination of 1.3 μm zero dispersion single mode fiber," in *Proc. IOOC-ECOC97*, Edinburgh, U.K., Sept. 1997, pp. 127–130.
[11] C.-Y. Kuo, D. Piehler, C. Gall, J. Kleefeld, A. Nilsson, and L. Middleton, "High-performance optically amplified 1550-nm lightwave AM–VSB CATV transport system," in *Proc. OFC'96*, San Jose, CA, Feb. 1996, pp. 196–197.
[12] E. Gertel, "Wide dynamic range optical link using DSSC linearizer," in *Proc. SPIE—The Int. Soc. Opt. Eng.*, vol. 2155, 1994, pp. 264–274.
[13] M. L. Farwell, W. S. C. Chang, and D. R. Huber, "Increased linear dynamic range by low biasing the Mach–Zehnder modulator," *IEEE Photon. Technol. Lett.*, vol. 5, pp. 779–782, July 1993.
[14] M. Y. Frankel and R. Esman, "Single-sideband suppressed-carrier optical modulator for wideband RF signal processing," in *Proc. OFC'98*, San Jose, CA, Feb. 1998, pp. 258–259.
[15] M. R. Phillips, "Amplified 1550-nm CATV lightwave systems," in *Proc. OFC '98*, San Jose, CA, Feb. 1998, pp. 22–27.
[16] W. I. Way, "Broadband hybrid fiber coax system and network technologies," in *Proc. OFC '99 Tutorial*, San Diego, CA, Feb. 1999, pp. 35–67.
[17] C. Y. Kuo and S. Mukherjec, "Clipping reduction for improvement of analog and digital performance beyond clipping limit in lightwave CATV systems," in *Proc. OFC '96* , Feb. 1996, Postdeadline PD 18.
[18] P. Y. Chiang, C. C. Hsiao, and W. I. Way, "Using precoding technique to reduce the BER penalty of an M-QAM channel in hybrid AM-VSB/M-QAM subcarrier-multiplexed lightwave systems," *IEEE Photon. Technol. Lett.*, vol. 10, pp. 1177–1179, Aug. 1998.

Frank S. Yang received the B.S. degree from the University of California at Berkeley, and the M.S. and Ph.D. degrees from Stanford University, Stanford, CA, all in electrical engineering.

He was a member of the Optical Communication Research Laboratory at Stanford University. His research field included DWDM systems, SCM optical systems, fiber nonlinearity, and optical parametric amplifiers. He is author or coauthor of 27 journal and conference papers. Over the past six years, he has worked in Northern Telecom, Hewlett-Packard, and Lucent Technologies. He is currently a Member of the Technical Staff at Ciena Corporation, Cupertino, CA.

Michel E. Marhic (M'79–SM'89) received the Diplome D'Ingenieur from Ecole Superieure D'Electricite, France, the M.S. degree from Case Western Reserve University, Cleveland, OH, and the Ph.D. degree from the University of California at Los Angeles (UCLA), all in electrical engineering.

He was on the Faculty of the Department of Electrical Engineering at Northwestern University, Evanston, IL, (1974-1998), and on sabbatical leaves at the University of Southern California (USC) (1979-1980), and Stanford University (1984-1985, and 1993-1994). He is currently Consulting Professor in the Department of Electrical Engineering at Stanford University. He is the cofounder of Holicon, Holographic Industries, and OPAL Laboratories. Over the past 25 years, his research has been in several areas of applied optics including: nonlinear interactions in plasmas; optical fiber measurements; hollow infrared waveguides; holography and phase conjugation; and fiber networks. Over the past ten years, his emphasis has been on optical communication systems and on nonlinear optical interactions in fibers. He is the author or coauthor of over 160 journal and conference papers and has been awarded eight patents.

Dr. Marhic is member of the Optical Society of America (OSA) and eminent member of Tau Beta Pi. In 1990–1991, he was recipient of the Ameritech Research Professorship from the Institute for Modern Communications.

Leonid G. Kazovsky (M'80–SM'83–F'91) as born in Leningrad, Russia, in 1947. He received the M.Sc. and Ph.D. degree in electrical engineering from the Leningrad Electrotechnical Institute of Communications, Leningrad, Russia, in 1969 and 1972, respectively.

He moved to Israel in 1973. From 1974 to 1984, (with a one-year interruption for active military service), he taught and was engaged in research at Israeli and United States universities. From 1984 to 1990, he was with Bellcore, Red Bank, NJ, doing research on coherent and WDM optical fiber communication systems. In 1990, he joined Stanford University, Stanford, CA, as a Professor of Electrical Engineering. He has published extensively in the areas of optical communications, applied optics, detection and estimation theory, and signal processing. He is the author or coauthor of more than 100 journal technical papers, of numerous conference papers, and of two books in 1978 and 1996, respectively.

Dr. Kazovsky has acted as a Reviewer for various EKE and EE Transactions, Proceedings, and Journals, as well as for funding agencies (the National Science Foundation, Energy research Council, etc.) and publishers (John Wiley and Sons, Macmillan, etc.). He currently serves (or has served) on Technical Program Committees of OFC, CLEO, SPE, and GLOBECOM, and is an Associate Editor of IEEE TRANSACTIONS ON COMMUNICATIONS, IEEE PHOTONICS TECHNOLOGY LETTERS, and of *Wireless Networks*. He is a Fellow of the Optical Society of America (OSA).